Evidence that the spectrin network and a nonosmotic force control the fusion product morphology in electrofused erythrocyte ghosts

Leonid V. Chernomordik and Arthur E. Sowers
Cell Biology Department, Jerome H. Holland Laboratory for the Biomedical Sciences, American Red Cross, Rockville, Maryland 20855

ABSTRACT The conversion of the membrane area in the "contact zones" shared by erythrocyte ghosts held in contact by dielectrophoresis into a fusion product by electrofusion was studied by both light and electron microscopy. Fusion products fell into two categories: (*a*) those with a freely expanding open lumen which ended in the "giant cell morphology" and with considerable internal vesicle membrane fragments, and (*b*) linear chains of polyghosts with long term stability but having planar diaphragms at the ghost–ghost junctions. Thin section electron microscopy showed each of these planar diaphragms to be a double membrane septum multiply-perforated with fusion pores. Heat and low ionic strength treatments known to denature or detach spectrin caused the stable planar diaphragms to dissolve, thereby quickly converting the polyghost chains to the giant cell morphology, thereby suggesting that spectrin restricts fusion zone diameter expansion if it is intact. Other indications suggest that the expansion of the open lumens appears to take place as a result of one or more membrane-specific forces with a nonosmotic origin but this tendency to expansion can be overcome if the spectrin network on only one side of a contact zone is intact.

INTRODUCTION

All membrane fusions must begin with two membranes in close contact. This contact, or "contact zone," must have some "fusion-permitting" average perpendicular distance between these two membranes and must extend over some finite but specifiable area. As fusion takes place, the two membranes undergo a poorly understood but possibly multistep structural rearrangement (Papahajopoulos et al., 1988; Blumenthal, 1987; Rand and Parsegian, 1986; Sowers, 1989; Chernomordik et al., 1987, for reviews), in which the membranes and the volumes surrounded by them become connected by at least one relatively narrow fusion pore (Sekiguchi et al., 1981; Zimmerberg et al., 1987; Breckenridge and Almers, 1987; Plattner, 1989; Monck et al., 1991). It has been reported (Sarkar et al., 1989; Zimmerberg et al., 1987; Spruce et al., 1989; Huang et al., 1990) that some fusion pores can close and open repeatedly or be stabilized near a radius of ~40–75 nm. If one of two fusing membranes is an enveloped virus then the nucleic acid load is not likely to pass though such a fusion pore unless it becomes substantially larger (Haywood, 1987).

Address correspondence to Dr. Sowers.
Dr. Chernomordik's permanent address is Frumkin Institute of Electrochemistry, Academy of Sciences of the USSR, 31 Leninsky Prospect, Moscow 117071, Union of Soviet Socialist Republics; his present address is National Institute of Child Health and Development, National Institutes of Health, Building 10, Room 6C101, Bethesda, Maryland 20892.
Dr. Sowers' present address is Department of Biophysics, University of Maryland School of Medicine, Baltimore, Maryland 21201.

If both of the prefusion membranes are cell plasma membranes, then the cell fusion process may continue if the diameter of the fusion pore increases to the point where it becomes unambiguously detectable by light microscopy and may finally end in a final fusion product which is a much larger and spherical or "giant" cell. Here we will use the term "giant cell morphology" to refer to such fusions of at least two cells into a large sphere. This is in contrast to fusions in which the final morphology is subspherical or has one or more fusion pores with diameters that cannot be resolved by light microscopy. Such fusion products have been described (Knutton and Bachi, 1980) and have been observed in what has been reported as nonlumen producing products of membrane electrofusion (Figs. 4–6 in Sowers, 1984).

In the present paper we used electrofusion, a protocol for artificially inducing fusion of membranes with an electric field pulse (Sowers, 1984; 1989; Zimmerman, 1982, for reviews), to fuse erythrocyte ghosts to study: (*a*) what happens as the contact zone converts to a fusion zone, and (*b*) the expansion of the fusion pore diameter until the giant cell morphology formed. We studied the changes in morphology of the contact zone of the ghost membranes of human and rabbit erythrocytes from just before the fusogenic pulse until such time after the pulse as the fusion product morphology became stable again. The fact that the membrane of erythrocytes is attached to a membrane skeleton network (Lux, 1979; Marchesi, 1985) which is specifically

0006-3495/91/11/1026/12 $2.00

sensitive temperature and ionic strength allowed us to find that the membrane skeleton plays a critical role in the stabilization of some fusion products. This study also led to the important finding that the nonlumen-producing class of erythrocyte ghost fusion product (see Figs. 4–6 in Sowers, 1984) is due to the presence of a fusion zone (see Fig. 10) which is a septum perforated by multiple fusion sites. The presence of this septum thus physically prevents the typical giant cell morphology from forming.

MATERIALS AND METHODS

Erythrocyte and ghost preparation

Rabbit erythrocytes were obtained from whole blood (15 ml) of New Zealand white rabbits by collection into vacutainers containing 0.3 ml of sodium citrate (1 M) as an anticoagulant. Human erythrocytes were obtained as packed cells from whole blood from the Chesapeake Region Blood Center. Rabbit and human erythrocyte ghosts (REG and HEG, respectively) were obtained by hypotonic lysis as follows. After washing the packed cells two times in isotonic sodium phosphate buffer (NaPi), at pH 7.4, with centrifugation at 300 *g*, 10 min, the supernatant and buffy coat were removed by aspiration and the soft pellet of the cells recovered for hemolysis by resuspension in 30 pellet vol of 5 mM NaPi (pH 8.5) for 20 min. The ghosts were then washed two times (10,000 *g*, 20 min) in 20 mM NaPi (pH 8.5). Pellets of this preparation of erythrocyte ghosts had a pink color. White pellets of erythrocyte ghosts were obtained by following the same procedure except that the hemolysis step (20 min incubation in 5 mM NaPi and then pelleting of ghosts) was repeated two times, one after another. Residual hemoglobin concentrations of pink and white REG were determined spectrophotometrically (Sowers, 1990) to be ~1.2% and 0.07%, respectively of that in the intact erythrocyte.

REG and HEG were stored as pellets in the 20 mM NaPi (pH 8.5) at 0–4°C for not more than 3 d until samples were withdrawn for the fusion assay. All stages of ghost preparation procedure described above were conducted at 0–4°C unless otherwise specified.

Some experiments used intact human and rabbit erythrocytes which were obtained from whole blood after two washes in isotonic NaPi (pH 7.4). Then cell pellets were resuspended in 20 vol of a buffer made of 0.25 M sucrose, 20 mM NaPi (pH 7.3).

The REG and HEG were labeled with 1,1'-dihexadecyl-3,3,3',3'-tetramethylindocarbocyanide perchlorate (DiI) as previously described (Sowers, 1988). DiI was obtained from Molecular Probes, Inc. (Eugene, OR). All other reagents were from Sigma Chemical Co. (St. Louis, MO).

Loading erythrocyte ghosts with protease inhibitors

Phenylmethylsulfonyl fluoride (PMSF) or *N-p*-tosyl-*l*-lysine chloromethyl ketone (TLCK) was loaded into the cytoplasmic compartment of the REG as follows. Each was added to 5 mM NaPi (pH 8.5) to make a final solute concentration of 1 mM in the REG pellet immediately after the hemolysis step. After 20 min of incubation in ice, enough 200 mM NaPi (pH 8.5), also containing the solute at 1 mM, was added to the sample to increase the buffer concentration to 20 mM and the REG were incubated 1 h at 30°C to reseal the pores. The REG were then washed two times in 20 mM NaPi but without the solute added.

Specific treatments of intact erythrocytes or erythrocyte ghosts

Aliquots (0.1–1 ml) of an REG suspension (pellet or 10× diluted pellet) were incubated: (*a*) at an elevated temperature (42 ± 0.5°C for 10 min in 20 mM NaPi, pH 8.5 unless otherwise indicated), and (*b*) at a low ionic strength (5 mM NaPi, 25°C, 2 h). At the end of incubation the suspension was transferred to ice. Intact rabbit erythrocytes in isotonic NaPi (pH 7.4) were identically treated. Phase contrast microscopy showed that the treatment described produced undetectable changes in the morphology of REG and intact cells.

Chambers

The "microslide" fusion chamber used to carry out the electrofusion experiments with observation by phase contrast and fluorescence microscopy was as previously described (Sowers, 1984). To study the ultrastructure of fusion products more than 15 min after the electrical treatment of ghosts we used a homemade bulk volume chamber (Fig. 1) with two wire electrodes having a diameter of ~1.0 mm and positioned with a 2-mm gap on opposite sides of the round plastic wall (diameter 3 mm). The sample volume contained by this chamber was 10 μl.

Generators

The equipment which provided the dielectrophoreis-inducing sine wave alternating current (60 Hz, AC, 15 V/mm) and the single fusogenic direct current (DC) exponentially decaying pulse was previously described (Sowers, 1989). In all experiments the decay half-time was 1.2 ms. In some experiments the sine wave AC used for dielectrophoresis had a frequency of 300 kHz instead of 60 Hz and was obtained from a BK Precision 3010 function generator (Maxtec International, Chicago, IL) coupled to a homemade amplifier with a voltage gain of 3. The parameters of applied AC and DC signals were monitored by means of a Tektronix (Beaverton, OR) T-912 storage screen oscilloscope.

Protocols

Unless otherwise indicated, the membranes were brought into contact through dielectrophoresis-induced pearl chain formation (Pohl, 1978) before the application of a single fusogenic electric pulse. The alternating electric field used for dielectrophoresis was 15 V/mm at 60 Hz, as previously described (Sowers, 1989). Each fusogenic pulse had a peak field voltage (V) which, when applied across the chamber length of 2 mm, generated a field strength (E = V/2 mm). Fusion yield assays were conducted at 20–24°C in 20 mM NaPi (pH 8.5) unless otherwise

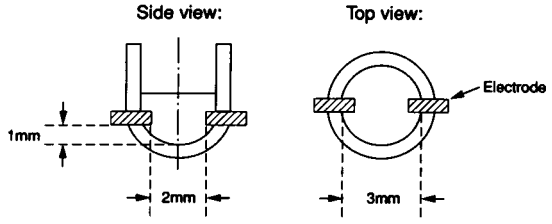

FIGURE 1 Plastic-walled chamber used to obtain preparative quantities of fused rabbit erythrocyte ghosts. Solder-tinned copper wire electrodes are sealed into holes in the wall with cement (see Methods).

indicated. For any experimental condition all ghost membranes were made from the same preparation. The only difference between the membranes was that one in 15 were DiI-labeled and the remainder were unlabeled. Fusion yields (FY) based on the DiI assay were calculated in "percent" from two categories of counts made after the pulse was applied: (*a*) single (i.e., unfused) fluorescent ghost membranes (N_s), and (*b*) two or more (i.e., fused) adjacent fluorescent ghosts (N_m) and use of formula $FY = [(N_m)/(N_s + N_m) \times 100$.

Phase contrast and fluorescence microscopy and micrography

All phase contrast and fluorescence light microscopy and micrography were conducted with a Zeiss Model 16 microscope with a Zeiss MC63 camera system (Carl Zeiss, Inc., Thornwood, NY) (electromechanical shutter and motor-driven film advance), and illumination from either a tungsten light source or epiillumination using a mercury lamp. The film used was Kodak technical pan film 2415 developed in Ektaflow (dilution 1:10) for 5–7 min, stopped, and fixed. Wires were connected to the push switch in the MC63 control panel which activated first the shutter and then the motor-driven film advance which brought unexposed frames of film into position for the next exposure. These wires were brought outside the MC63 control panel and, together with control wires which triggered the pulse generator, connected to a set of time delay relays which, altogether, permitted image exposures 0.25 s long to be recorded automatically on a new frame of unexposed film every 1.0 s. The relays could be adjusted to allow any specific frame to be exposed at any desired time after the fusogenic pulse was triggered. These intervals were measured and monitored on a storage-screen oscilloscope.

Measure of membrane area lost to internal vesiculation during fusion

Erythrocyte ghosts in pearl chains were fused to obtain fusion products with diameters of 20–30 μm. These fusion products were aligned again into pearl chains and fused again with a single pulse. Micrographs were made both before the pulse and after the fusion product morphology reached its final shape and size. Images of the two spherical fusion "substrates" and the single fusion "product" in the micrograph were cut along the edges of the image. Using a mass balance, the weight of a unit area of photographic paper was compared with the area of the cut-out images with algebra to calculate the ghost membrane surface area and thus determine how much substrate membrane is lost to vesiculation (see Discussion).

Thin section electron microscopy of fusion products

The ghosts of rabbit erythrocytes were fused by the application of a single DC pulse of 0.4 kV/mm to ghosts aligned by AC (15 V/mm, 300 KHz) in the bulk volume chamber (Fig. 1). One minute after the pulse the suspension of fusion products was transfered from the chamber to a plastic tube containing 0.25% glutaraldehyde in 20 mM NaPi (pH 8.5). Nine additional volumes of ghosts were subjected to this protocol to produce a total of 0.1 ml volume of the fusion products. After 20–40 min of prefixation in 0.25% glutaraldehyde, the ghost membranes were further fixed in 2.5% glutaraldehyde in the same buffer overnight at 0–4°C. The glutaraldehyde-fixed ghosts were washed and then post-fixed in 1% OsO_4 for 30 min at 20–22°C. After a wash in water, the ghost membranes were prestained with uranyl acetate for 20 min and washed with H_2O and carried through dehydration in ethanol and infiltrated with epoxy in graded stages and then polymerized at 60°C for 48 h. Thin sections were cut with a diamond knife on a LKB Ultratome and examined and micrographed with a HU 12 electron microscope (Hitachi Science Instruments, Mountain View, CA).

RESULTS AND DISCUSSION

Changes in the contact zone as induced by the pulse and as observed by phase contrast light microscopy

Application of the alternating electric field to the suspension of rabbit erythrocyte ghosts (REG) or human erythrocyte ghosts (HEG) caused the ghosts to come into contact by pearl chain formation with the chain axes parallel to the electric field lines. As viewed in fluorescence optics, the application of a DC pulse with a strength E = 0.25–1.0 kV/mm and 1.2-ms decay half-time (for REG) to the pearl chains of ghosts resulted in fusion as evidenced by a lateral diffusion of the DiI from the originally labeled membranes to at least one adjacent but originally unlabeled membrane. In phase contrast optics, however, the pulse caused the morphology and appearance of the membranes in and near the contact zone to change to a "fusion zone" morphology which can best be described as having an optically dense planar area or diaphragm shared by two adjacent membranes which expands in diameter with time (Figs. 2 and 3). This was consistent with previous observations (Sowers, 1984; 1988). However, the DC pulse amplitude required to initiate DiI redistribution between HEG was much higher than that for REG. The minimum pulse field strength required to induce the optically dense diaphragm-type fusion zones, by phase optics (Fig. 2) from contact zone between HEG ($E > 0.85$ kV/mm), was also higher than that for REG ($E > 0.25$ kV/cm).

If one ghost in a pearl chain contained enough residual hemoglobin to be detectible by phase optics (Fig. 2, *arrow*), then the development of the diaphragm-type fusion zone upon pulse application was accompanied by the diffusion of hemoglobin from the hemoglobin-containing ghost to the adjacent empty ghost. Separate experiments using DiI-labeled erythrocyte ghosts with high levels of residual hemoglobin and unlabeled pink or white ghosts as fusion partners showed that hemoglobin was found to have moved (contents mixing) *in each and every case that DiI also became redistributed* (membrane mixing). Examination of more than 1,000 of these fusion zones in fused chains of ghosts containing a mixture of unlabeled and DiI-labeled ghosts (10:1) showed that, regardless of fusion zone diameter, fluorescence had diffused laterally to at least one adjacent unlabeled membrane. It should be noted that, as relevant to the

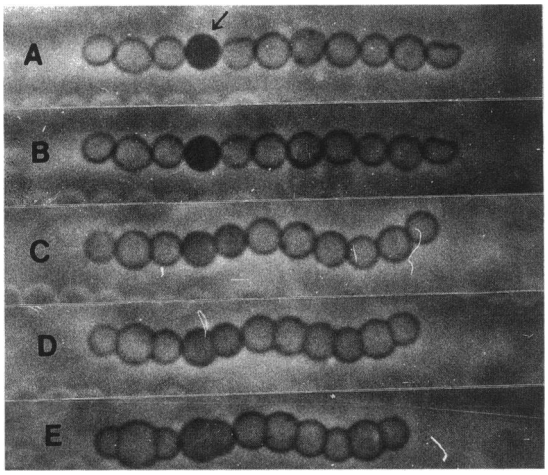

FIGURE 2 Phase optics light micrographs showing time dependent changes during electrofusion of control (no heat treatment) rabbit erythrocyte ghosts held in pearl chains. Changes followed the application of a single electric field pulse (E = 0.3 kV/mm, decay half time = 1.2 ms). The alternating current, used to hold the ghosts in the pearl chain, was turned off 5 s after the pulse. Note: (1) the relatively slow movement of hemoglobin in a "dense" ghost (*arrow*) to all "transparent" ghosts located to the right of it, and (2) contact zones where adjacent ghosts come into contract with each other expand in diameter leaving behind planar diaphragm fusion zones (cf Figs. 3, 5, 8) between each pair of fusion partners. Interval between micrograph and pulse: (*a*) before pulse; (*b*) 0.25 s after; (*c*) 9 s after; (*d*) 15 s after; and (*e*) 47 s after.

question of assay validity, a previous study showed that all fusion events could be rigorously determined with fluorescence optics usind DiI as a membrane mixing label (Sowers, 1988). That study also showed a discrepancy involving an excess number of contents mixing

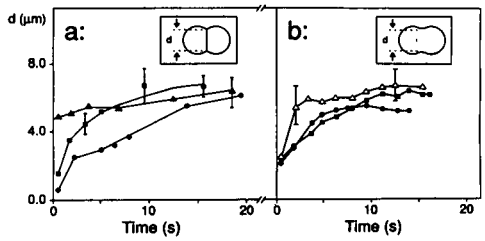

FIGURE 3 Average diameter, d, of fusion zones as a function of fusogenic pulse strength and time after the fusogenic pulse as measured from phase optics light micrographs (see text): (*a*) planar diaphragm fusion zones (cf *inset* and Fig. 2) in control (no heat treatment) rabbit erythrocyte ghosts; (*b*) in freely-expanding open lumen fusion zones (cf *inset* and Fig. 5) of heat-treated membranes (see text). Each point is measure of 10–16 fusion zone diameters. Bars are one standard deviation. Alternating current was turned off 5 s after the pulse. Electric field pulse (decay half time of 1.2 ms) strengths (E in kV/mm): (●), 0.3; (■), 0.4; (▲), 1.0; and (△), 0.7.

events over membrane mixing events. However, the discrepancy was hypothesized to be due to an electro-osmosis-induced artifact which is now confirmed (Dimitrov and Sowers, 1990*a*). Thus the excess contents mixing events are likely to be caused by pulse-induced (rapid = 10–100 ms time scale) electroosmosis in electropores (Dimitrov and Sowers, 1990*a*). Whereas this could be easily factored out with an added step in the protocol, the contents mixing label would then not be a measure of true contents mixing but would simply be a visual label which would identify membranes as fused on the basis of physical attachment (Sowers, 1988) rather than the membrane fusion criterion based on actual contents mixing. True contents mixing would have to be followed, for example, through a (slow ≃ 30 s) diffusion-through-a-lumen observation such as shown in Fig. 2). However contents mixing labels are usually soluble macromolecules which have now been shown to affect electrofusion yields (Sowers, 1990) through an unknown mechanism. Thus there is a one to one absolute correspondence between contents mixing, membrane mixing, and irreversible attachement as rigorous criteria (see Sowers, 1988) for membrane fusion.

We did not see the development of a planar diaphragm from the contact zone if a fusogenic pulse was applied before, instead of after, close membrane–membrane contact was established. In this experiment a pair of ghosts which were close spaced (2–4 μm) and on or near the electric field axis used for both alignment and induction of fusion was selected. Then the AC field was applied to the suspension to cause the ghosts to move towards contact. A DC pulse of 1 kV/mm was applied just 1–2 s before they actually came into contact.

The ultrastructure of the fusion zone

Thin section electron micrographs (Fig. 4) through fusion zones shared by REG in a pearl chain showed that these diaphragms are composed of double membrane "septums" with many perforations (=fusion sites or passages in the zones which border the two cytoplasmic compartments) (see Figs. 2, 3, and 8). Thus, the electrofusion of the membranes caused the formation of a sievelike system of fusion pores in the fusion zones. The number of fusion pores range from three to more than 10 in each fusion zone and have minimum diameters of ~0.1 μm.

The electron micrographs showed not only that these sites exist but they have long term stability (up to 48 h at 0–4°C) and survive conventional processing for thin section electron microscopy. The fact that the overall morphology by electron microscopy (Fig. 4) is identical to that observed by light microscopy (Fig. 2) suggests that this is not an artifact of fixation and preparation for

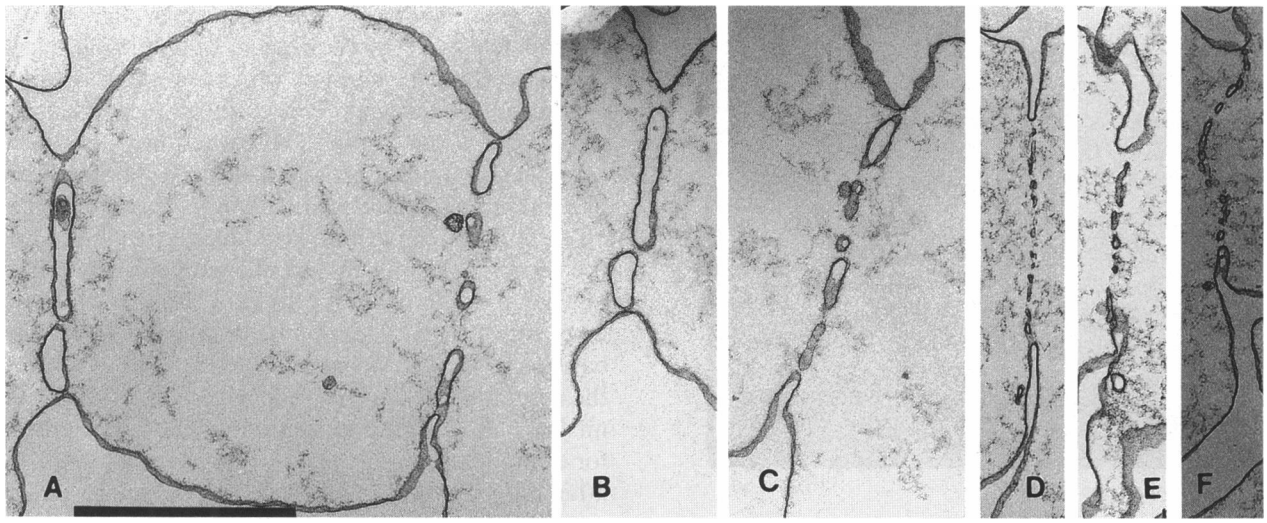

FIGURE 4 Thin section electron micrographs of stable planar diaphragm fusion zones induced with a single pulse (E = 0.4 kV/mm, decay half-time = 1.2 ms) in rabbit erythrocyte ghosts held by dielectrophoresis in a pearl chain: (*a*) two stable diaphragm fusion zones shared between three erythrocyte ghosts in a pearl chain (oriented left-right); (*b* and *c*) same two fusion zones, respectively, as in (*a*) except section plane is shifted 0.15 um indicating large diameters of fusion pores, (*d–f*) three other representative examples of stable planar diaphragm fusion zones showing hints of periodicity, heterogeneity in fusion pore diameter. Line scale is 3μm; all magnifications identical.

thin section electron microscopy. Moreover, the fact that the morphology in Fig. 4 is identical to that found in freeze-fracture electron microscopy of virus-induced fusion of erythrocytes (Fig. 17 in Knutton, 1977) is additional evidence that our observation is not an artifact. There is a hint of periodicity in the spacing of these fusion sites in the diaphragms which suggests that the electric field may induce in the membrane a force which propagates in the plane of the membrane and accumulates at multiple locations which become fusion sites. The complex ultrastructure shown in the electron micrographs also suggests that rearrangements in membrane topology may also have taken place. Because open lumen fusion zones lead, in a self-completing process, to the giant cell morphology, it appears that the membranous diaphragm produces a restraining force which prevents the giant sphere morphology from forming.

Effect of heat treatment

Fig 5 shows, in phase optics, electrofusion of pink REG that were treated by incubation for 10 min at 42°C in 20 mM NaPi to disrupt the spectrin network. Before the DC pulse the ghost pearl chains had the same appearance as the chains formed from control (=unheated) ghosts (Fig. 2, *a*). The application of a fusogenic DC pulse to heat-treated ghosts in pearl chains caused a rapid (seconds) conversion of the contact zones directly into one of two classes of fusion product. The first class had the same stable, optically dense flat areas or diaphragms as seen in Fig. 2 whereas the second class had open lumens (hourglass constrictions) with diameters that freely and continuously increased until the giant cell morphology was reached (Fig. 5). However, the stable planar areas in the fusion products had qualitatively smaller diameters in Fig. 5, *b–d* than corresponding locations in Fig. 2, *e*. The proportion of adjacent ghosts in the chains which converted to the giant cell morphology was generally proportional to both the number of ghosts in the pearl chains and the amplitude of the fusogenic electric pulse (data not shown). The heat treatment of REG thus caused a change in membrane properties that permitted the giant cell morphology to form instead of the formation of irreversible chains with stable diaphragm fusion zones.

The production of the diaphragm-type fusion zone still occurs in a subpopulation of membranes which have been treated to alter spectrin. Note in Fig. 5 that despite the many open lumen fusions, many junctions remain which cannot be identified as either a contact zone or a diaphragm-type fusion zone unless either the "physical attachment criterion" (Sowers, 1988; 1989) is tested by removing the dielectrophoretic force and allowing unfused contact zones to dissociate by Brownian motion or using a fluorescent membrane label to measure membrane mixing.

Except for the data obtained with the highest and lowest pulse strength, the rates of diaphragm diameter increase (Fig. 3, *a*) and open lumen diameter increase (Fig. 3, *b*) were roughly similar, within experimental

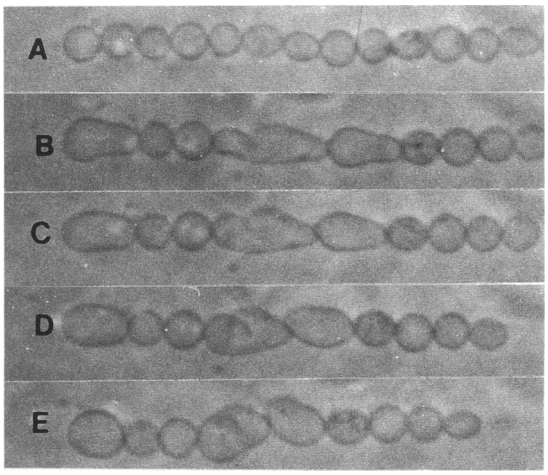

FIGURE 5 Phase optics light micrographs showing time dependent changes during electrofusion of heat-treated (42°C, 10 min) rabbit erythrocyte ghosts held in pearl chains. Changes followed application of a single electric field pulse (E = 0.4 kV/mm, decay half-time = 1.2 ms). The alternating current, used to hold the ghosts in the pearl chain, was left on throughout the sequence. Note that contact zones are converted to fusion zones which expand in diameter as open lumens (i.e., without leaving behind optically dense planar diaphragm fusion zones, cf Fig. 2, 3, 8) between each pair of fusion partners. Interval between micrograph and pulse: (*a*) before pulse; (*b*), 0.25 s after; (*c*) 1.5 s after; (*d*) 4.75 s after; and (*e*) 9.25 s after.

error, in the first 10–15 s after the pulse. Fusions between pairs of control ghost membranes very rarely (<0.2% of all fusion zones) led to fusion products having the giant cell (spherical) morphology. In other words, most (>99.8%) of the fusion products were in the form of linear chains of spherical ghosts with optically dense flat areas at the junctions (Fig. 2, *e*). The application of additional DC pulses to a chain of ghosts fused by a previous pulse never resulted in the giant cell morphology unless a series of pulses were used with field strengths of at least E = 0.9–1 kV/mm. The average rate of diameter increase of the open lumens (see *inset*, Fig. 3, *b*) as a function of time after application of 0.4 kV/cm was independent of whether the REG were white or pink (data not shown). Compared to standard deviations in the data, the speed with which the fusion zone diameter increases, regardless of whether in the form of optically dense diaphragms or open lumens, is, with two exceptions, relatively independent of both spectrin integrity and field strength of the fusogenic pulse (Fig. 3). The two exceptions were: (*a*) a more rapid diaphragm diameter expansion, but only in the first 1 s, for E = 1.0 kV/mm (Fig. 3, *a*), and (*b*) a slower expansion throughout the measurement interval (20 s) for E = 0.3 kV/mm compared to E = 0.4 kV/mm. Open lumen diameter expansion (Fig. 3, *b*) was also more rapid (in the first 2 s) for 0.7 kV/mm than for either 0.3 or 0.4 kV/mm which were each essentially identical. The basis for these differences is not known, but interactions with other membranes in pearl chains may influence the processes. Note that the fusion zone diameter continues to increase in a very slow (>1 min) process in the spectrin-damaged membranes until the giant sphere morphology is reached but would not be apparent from the data in Fig. 3. The highest rate of expansion always appears to be in the first 1.0 s and ranges over 1–4 μm/s. In an earlier paper (Sowers, 1985) the rate of expansion was measured in fused intact human erythrocytes and found to range over 0.15–0.84 μm/s, suggesting that the forces involved are considerably different in the two systems.

Effect of low ionic strength treatment

Once the planar fusion zones stopped increasing in diameter (20–60 s after the pulse), their appearance was both stable and independent of the presence of AC for up to 48 h after the pulse application if they were stored at 0–4°C. However, a 10 min incubation of such chains of fused ghosts at 20–22°C in 5 mM NaPi, pH 8.5, caused the formation of the giant cell morphology (i.e., each stable chain of ghosts converted into a giant sphere) without any trace of the original stable flat fusion zone.

Further characterization of the heat treatment effect

Incubation of heat-treated REG at 5°C for three d before the electrofusion experiments did not prevent the formation of the giant cell morphology and thus showed that the effect of the heat treatment was irreversible. A heat-treatment temperature of 40°C, instead of 42°C, caused fewer giant cell morphologies to be formed. The giant cell morphology was not found at all if the heat treatment was carried out at 38°C. Conversely, incubation of REG for 10 min at temperatures ≥45°C resulted in the vesiculation of membranes and a large decrease in fusion yield. Chains of fused REG with stable diaphragm fusion zones converted to giant cell morphologies if they were subsequently heated in the chamber for 10 min at 42°C with the alternating current field on all the time. Heating REG to 42°C while being held in pearl chains never caused giant cell morphologies unless a fusogenic electric pulse was applied.

Effect of ionic strength on temperature threshold of heat treatment effect when intact erythrocytes are electrofused

To determine how a higher buffer strength affects the temperature threshold at which the heat treatment

effect takes place, fusions were induced in intact rabbit erythrocytes which were incubated in isotonic sodium phosphate buffer (pH 7.4) for 10 min at 42°C and then electrofused in 220 mM sucrose, 20 mM sodium phosphate buffer (pH 7.4). These were observed to show the same phenomenology as control (=unheated) cells. In other words, the chains had stable flat optically dense fusion zones. However, incubation of cells at 47°C for 10 min allowed the giant cell morphology to form after pulse application. The formation of the giant cell morphology in this case was accompanied by partial or almost complete release of hemoglobin by the intact erythrocytes. We also observed that the heat treatment appears to stabilize the REG against electrically-induced hemolysis: the application of a 0.4 kV/mm pulse (1.2 ms decay half time) to intact rabbit erythrocytes in pearl chains results in hemolysis of ~85% of control (=unheated) cells in comparison with 25% of heat-treated cells. When the temperature of the heat treatment was 50°C the membranes of the rabbit erythrocytes vesiculated.

Heat treatment of intact rabbit erythrocytes at 42°C or 46°C in isotonic sodium phosphate buffer (pH 7.4) for 10 min followed by preparation of ghosts which were then assayed for FY in 20 mM sodium phosphate buffer (pH 8.5) using a fusogenic pulse in the range 0.3–0.6 kV/cm did not lead to the giant cell morphology for 42°C but did for 46°C. A similar result was found for HEG except that the field intensity required for fusion of heat-treated HEG was significantly higher than that for fusion of heat-treated REG (i.e., 1 kV/mm instead of 0.3 kv/mm, respectively, for ~50% fusion yield). A similar quantitative difference between ghosts of human and rabbit erythrocytes was observed as well for the electrofusion of unheated ghost membranes studied by phase-contrast microscopy (see above) and by the DiI-based fusion assay (Sowers, 1989).

The basis for the heat treatment effects is likely to be disruption of the spectrin network

Effects of heat treatments on erythrocyte membranes have been extensively studied. Erythrocyte (Rakow an Hochmuth, 1975; Mohandas et al., 1976; 1978, de Bruijne and van Steveninck, 1979) and erythrocyte ghost (Heath et al., 1982) deformability decrease dramatically after heat treatment of human erythrocytes in the range 45–50°C for 10 min. Other reports show that >35–37°C spectrin is partially denatured (Cassoly et al., 1980) and spectrin tetramers dissociate into dimers in a simple thermodynamic equilibrium (Marchesi, 1985; Ungewickle and Gratzer, 1978). Furthermore, a calorimetric transistion over the range of 43–54°C (with a peak at 49.5°C) was shown to be exclusively due to spectrin (Brandts et al., 1977). The fact that the temperature of heat treatment used in our study (42°C) which had maximum effects was slightly lower than some of the heat treatment temperatures (45–50°C) from the other reports may have been due to the fact that our medium was 20 mM NaPi whereas the media used in the previous papers was isotonic NaPi, PBS, or another more complex buffer. This possibility was supported by separate experiments which showed that the threshold temperature of the heat treatment effect increased up to 46° when we subjected intact rabbit erythrocytes to the heat treatment in isotonic sodium phosphate buffer instead of erythrocyte ghosts in 20-mM buffer. The change induced by the heat treatment is irreversible but is not related to the protease activation that has been reported to play a role in fusion process (Ahkong et al., 1980; Lang et al., 1984; Ohno-shosaku and Okada, 1989) because the presence of serine and cysteine proteinases inhibitors PMSF and TLCK during the heat treatment had no effect. It is therefore concluded that the heat treatment effect on fusion product morphology is through an alteration in spectrin.

The basis for the low ionic strength effect is likely to be a disruption of the spectrin network

Giant cell morphologies were found after the application of the fusogenic pulse when REG were incubated for two h at 25°C in 5 mM sodium phosphate buffer, pH 8.5 (but not at either 5° or at 25°C in 20 mM buffer) (Fig. 6). These observations are consistent with known

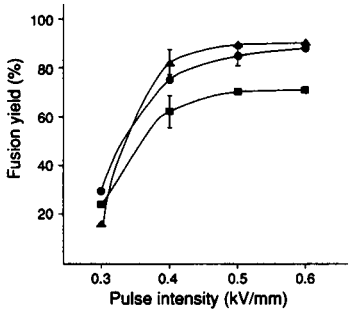

FIGURE 6 Field strength (E) dependent, DiI-based fusion yields as induced with a single pulse (half-time of 1.2 ms) in control (no heat treatment) white rabbit erythrocyte ghosts to different posthemolysis washing protocols (pH 8.5): (▲), washing in 20 mM NaPi and storage at 0–4°C; (●), washing in 20 mM NaPi followed by a 2-h incubation at 25°C in 20 mM NaPi and storage at 0–4°C; (■), a 2-h incubation at 25°C in 5 mM NaPi followed by washing in 20 mM NaPi followed by storage at 0–4°C.

factors which can disrupt the spectrin network (Marchesi, 1985).

Fusion of heat-treated ghost with a control (=unheated) ghost

This experiment was designed to determine if both or only one spectrin network had to be disrupted for open lumen formation to occur after fusion. It required two parts. First, heat-treated REG wee labeled with DiI and mixed (10:1) with control REG (=unheated and unlabeled). Second, and as a control for the first part, the reciprocal experiment contained a 10:1 ratio of heat-treated, but unlabeled, membranes mixed with unheated DiI-labeled membranes. In both cases only the contact zones between fluorescent and nonfluorescent membrane were examined after the pulse. They were examined for two criteria: (*a*) fluorescence transfer (=fusion) across the junction, and (*b*) open lumen or planar diaphragm formation. The result was that, after the application of a 0.5 kV/mm fusogenic pulse, wherever fusion was demonstrated by fluorescence transfer it was never accompanied by the formation of the giant cell morphology. This suggests that the force causing the increase in the diameter of the open lumens is still weaker than the restraining force present on only one side of the stable flat diaphragm and would have to be due to intact spectrin. This is consistent with the widely held understanding that spectrin forms a continuous latticelike network attached to the membrane at anchor points (Lux, 1979; Marchesi, 1985).

Fusion product size and loss of fusion product membrane area to vesiculation

Measurements showed that the fusion products had 12.3 ± 5.8% (nine measurements) less total membrane area than in the fusion partners (see Fig. 7, 8). The generation of multiple fusion sites in the fusion zones was followed by fragmentation of the membrane in the fusion zone into vesicles which resulted in loss of some part of membranes area to the interior of the membrane enclosed volumes (Figs. 7, 8). The comparison of the areas of membranes of heat-treated REG before (the sum of the areas of surfaces of both fusion partners) and after fusion (the surface area of the fusion product) has shown that the formation of giant ghosts is in fact, accompanied by a loss of ~12% of total prefusion membrane area. The presence of membrane fragments inside the giant ghosts (Fig. 7) resembles the observation of analogous membrane fragments found inside electrofused mitochondrial inner membranes (Sowers, 1983) and in fused plant protoplasts (Vienken et al., 1983). It should be noted, however, that the process reported by Vienken et al. (1983) occurred in viable cells and occurred over a much longer time scale and thus, while it may be a similar process it may not be related to our observation in terms of cause and effect. It is also significant that the distribution of membrane fragment diameters in the present paper and in Sowers (1983) are small and similar in size distribution. Thus, the fragmentation of membrane area as the diaphragm-type fusion zone disassembles into vesicles may be a general property of electrofusion along with formation of the giant spherical fusion products. On the other hand, the heat and low ionic strength treatments used in the present study to promote giant ghost formation are also known to facilitate spontaneous membrane vesiculation (Elgsaeter et al., 1976; Mohandas et al., 1978). Thus, it may be that treatment-modified skeletons will promote giant ghost

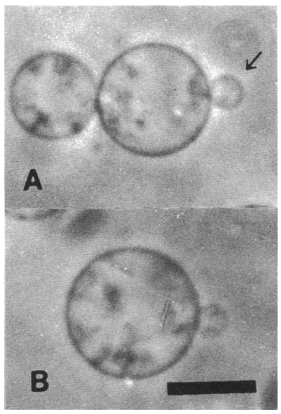

FIGURE 7 Large spherical fusion products of repeated fusion of smaller fusion products: same membranes, before (*a*) and after (*b*) pulse (scale = 15 μm). Single unaffected ghost at arrow. Alernating current left on at all times and four applications of electric field pulses.

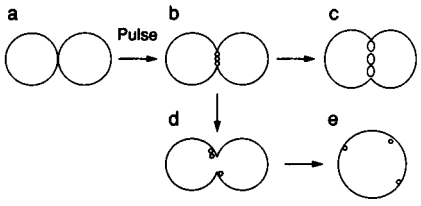

FIGURE 8 Electrofusion in rabbit erythrocyte ghosts as it depends on treatments known to affect spectrin: (*a*), pair of ghost membranes before fusogenic pulse; (*b*), unstable fusion zone with unknown ultrastructure increases in diameter until new equilibrium is reached with stable planar diaphragm type fusion zone at (*c*) or fusion product with the "giant cell morphology" at (*e*). Multiple fusion sites evidently become small vesicles with inverted asymmetry (*d*), as planar diaphram dissolves, which eventually aggregate or bind to inner surface of large fusion product membrane (see Fig. 7).

formation by the facilitation of the loss of membrane area that is a necessary condition of fusion pore expansion. All of these observations suggest, in turn, that as yet unanalyzed latent but nonosmotic forces may exist in the erythrocyte membrane and play significant roles in the topological transformation of membranes during membrane fusion.

Very large diameter fusion products and the pulse field strength needed to obtain them

Spherical shaped membrane fusion products with diameters up to at least 400 μm could be easily obtained by repeated fusion of already fused membranes. The larger the diameter of the fusion product, however, the more vesicular membrane material was observed bound to the inner surface of the ghost membrane. The intensity of the DC pulse required to induce fusion always decreased with an increase in the diameter of the fusion partners. The electrofusion of REG shown in Fig. 7, *a* to the fusion products in Fig. 7, *b* required a fusogenic DC pulse with $E = 75$ V/mm be applied two membranes (~25-μm diameter each) in contact to induce fusion. In this case a fourfold increase of the membrane fusion product diameter was accompanied by a more than threefold decrease of pulse field intensity for fusion. This is consistent with the expectation that larger membrane voltage drops will be produced for the same intensity of bulk electric field if larger diameter spherical membranes are used and is based on the theoretically derived equation $V = 1.5Er[\cos(\theta)]$, where V is transmembrane voltage induced at the poles by an external field, E, in a spherical-shaped membrane with radius, r, and θ is the angle between the field direction and the radius vector to the point on the sphere, as from numerous authors (Fricke, 1953; Teissie and Tsong, 1981).

The origin of the force which causes expansion of the fusion zone

"Membrane" fusion is now commonly distinguished from "cell" fusion in terms of (*a*) contents mixing and membrane mixing, and (*b*) giant cell formation, respectively (see Fig. 8). In all cases, the volume enclosed by the fused partners must increase at least somewhat as the fusion zone diameter increases and comes to final equilibrium. Water must enter the enclosed space. This change must be driven by forces. One popular origin is osmotic forces. If the interior (cytoplasmic) space is hypertonic with respect to the exterior, then an influx of water will have the effect of swelling the membrane and increase membrane tension. This can drive the increase in the fusion zone diameter. Observations in other systems which support this picture include contents mixing only after postfusion swelling (Wojcieszyn et al., 1983), colloid osmotic swelling of intact erythrocytes after electric field pulses (Sowers, 1985; Tsong, 1989) and osmotic swelling which commonly preceeds cell fusion (reviewed by Lucy and Ahkong, 1986; Lucy and Ahkong, 1988). The fact that the membrane/cell fusion is still not well understood is illustrated, for example, by outright claims that in a particular system osmotic forces are not involved (Pritzen and Herrmann, 1988; Hermann et al., 1988) despite the facts that: (*a*) earlier contrary evidence was quite good (Knutton and Bachi, 1980; Sekiguchi et al., 1981), and (*b*) the claims of the 1988 papers were not based on assays which would distinguish between membrane vs. cell fusion. A more detailed discussion of the osmotic origin of these forces is, however, beyond the scope of this paper.

In our studies, the forces due to osmotic pressure differences could be demonstrated when placing the REG in a hypertonic sucrose medium caused a slowing of the "rounding up" stage. This also suggested that the membrane still retained some permeability barrier to sucrose. Because the residual hemoglobin in the erythrocyte ghosts was <1% of that in an intact cell, the corresponding forces due to osmotic pressure differences should be much lower than in intact cells which are used in many studies. Residual hemoglobin concentrations in the pink and white ghosts, respectively, were either 1.2% or 0.07% of the total hemoglobin concentration in the intact red blood cell but showed no measureable effect on the rate of diameter increase in the fusion zone (data not shown) although this difference was shown to have a strong effect on fusion yield (Sowers, 1990). It is possible that an osmotic pressure difference could be generated by products of denaturation and degradation of membrane proteins or other residual soluble proteins which are released from the inner surface of the erythrocyte ghost during the heat treatment to the cytoplasmic space of erythrocytes or erythrocyte ghosts. This could increase the internal osmotic pressure and promote swelling after electroporation for heat-treated ghosts. However, this possibility is also unlikely because an additional stage of osmotic lysis after heating would be expected to release additional residual hemoglobin molecules and any other similar sized soluble molecules from initially pink ghosts but this had no effect on formation of the giant cell morphology upon fusion. Therefore the forces which expand the fusion zone are unlikely to be due to osmotic pressure effects.

Another origin of the force which can increase the fusion zone diameter includes an expanding or "pushing" force from the planar diaphragm, as it grows in diame-

ter, or a "pulling" force which originates from a curved membrane that has internal tension or stress (Monck et al., 1991). The fact that the giant cell morphology is the result when an open lumen fusion zone is created, by, for example, a heat or low ionic strength treatment (either before or after electrofusion), suggests that the planar diaphragm is a structure which actually restrains the expansion of the zone rather than assists it.

Pellets of ghost membranes obtained in the normal (wash-hemolysis-wash) erythrocyte ghost preparation were pink in color. If the pink REG were incubated at 42°C for 10 min in 20 mM buffer, and then subjected to an additional wash (5 mM) during hemolyis, then pellets were white in color. However, neither the introduction of a hemolytic hole in the plasma membrane of the heat-treated REG, which would allow molecules up to at least the size of hemoglobin to escape, nor the additional wash, inhibited the formation of the giant cell morphology. Hence, even the residual hemoglobin in pink ghosts is unlikely the basis for an osmotic force sufficient to cause the fusion zone expansion.

The fact that the heat treatment could be applied to control REG after they were fused to each other and still cause the flat planar diaphragm in the fusion zone to disappear and allow the giant cell morphology to form is also consistent with the notion that the force causing giant cell formation is overcome by a stronger restricting force when the stable diaphragm is present. Moreover, this fact suggests that both forces are independent of the fusogenic electric pulse but dependent on membrane properties.

The delay between the pulse and evidence of fusion

Whereas the time needed for the pulse voltage to achieve its peak is a fraction of a microsecond, the time needed for this voltage to decay out of existence ($<1\%$ field strength after eight 1.2 ms decay halftimes) ~ 10 ms. However the moment when the fusion event process begins and ends is unclear. It must occur at some instant before the consequences are observable. The earliest moment that fusion can be detected by phase optics is when an increase in the diameter of the open lumens is clearly visible by phase optics (Figs. 3 and 5). These are seen to appear no later than 0.25 s after the pulse in Fig. 5 and, certainly, no later than 2.0 sec after the pulse in Fig. 3, *b*. Another recent paper from this laboratory (Dimitrov and Sowers, 1990*b*) reported reproducible delays or time intervals between the moment of application of a fusogenic pulse and the earliest moment at which fluorescence could be detected in the originally unlabeled adjacent membrane. These delays, which were correlated with aqueous viscosity of the buffer, temperature, and electric field characteristics, always ranged from 0.3 to 4 s, depending on parameters, and resembled delays seen in fusion of viral envelopes with plasma membranes (Clague et al., 1990; Morris et al., 1989). Interpolating from data in Fig. 5 of Dimitrov and Sowers (1990*b*) with the data in Figs. 5 and 3, *b* of the present paper lead us to conclude that fusion can be detected by phase optics before it can be detected by lateral diffusion of a fluorescent dye from an originally labeled membrane to an adjacent membrane in a pearl chain.

Summary

It was reported in an earlier paper from this laboratory that fusions took place in two catogories: (*a*) with, or (*b*) without forming an open lumen visible by phase optics (see Figs. 4–6 of Sowers, 1984) and it was concluded in that paper that fusion yield calculated from counting only the lumen-producing fusions (i.e., by phase optics) would underestimate total fusion yield which would be a sum of both nonlumen and lumen-producing fusions. This paper: (*a*) further clarifies the nature of the two classes of fusion (Fig. 8), and (*b*) establishes a physical basis for the nonopen lumen fusion zones. Visible lumens and nonlumen fusion events in Sowers (1984) correspond to the "open lumen" fusion zone and the "optically dense diaphragm" fusion zone, respectively, in the present paper. A previous study of the effect of a 50°C heat treatment on electrofused erythrocytes reported a similar result but did not characterize its nature or rigorously analyze its origin (Glaser and Donath, 1987). It is also concluded that (*a*) the effects of heat and low ionic strength treatments described in the present paper, (*b*) the absence of demonstrable sources for osmotic pressure differences, and (*c*) the absence of a large difference in the rate of increase in the diameter of the fusion zone in planar diaphgrams compared to open lumens, reflects forces which are less likely to have an osmotic pressure origin but rather more likely to a latent tension or stress in the membrane itself.

Expert technical and electron microscopy assistance from Ms. M.-S. Cho is gratefully appreciated.

Supported by Office of Naval Research grant N00014-89-J-1715 to Arthur E. Sowers.

Note added in proof: Attention is called to the very interesting and relevant paper by Song, L., Q. F. Ahkong, G. Georgescauld, and J. A. Lucy. 1991. Membrane fusion without cytoplasmic fusion (hemifusion) in erythrocytes that are subjected to electrical breakdown. *Biochim. Biophys. Acta.* 1065:54–62.

Received for publication 15 February 1991 and in final form 22 May 1991.

REFERENCES

Ahkong, Q. F., G. M. Botham, A. W. Woodward, and J. A. Lucy. 1980. Calcium-activated thiol-proteinase activity in the fusion of rat erythrocytes induced by benzyl alcohol. *Biochem. J.* 192:829–836.

Blumenthal, R. 1987. Membrane fusion. *Curr. Top. in Membr. and Transp.* 29:209–254.

Brandts, J. F., L. Erickson, K. Lysko, A. T. Schwartz, and R. D. Taverna. 1977. Calorimetric studies of the structural transitions of the human erythrocyte membrane. The involvement of spectrin in the A transition. *Biochemistry.* 16:3450–3454.

Breckenridge, L. J., and W. Almers. 1987. Final steps in exocytosis observed in a cell with giant secretory granules. *Proc. Natl. Acad. Sci. USA.* 84:1945–1949.

Cassoly, R., D. Daveloose, and F. Leterrier. 1980. Spin labeling of human spectrin. Effects of temperature, divalent cations and reassociation with erythrocyte membrane. *Biochim. Biophys. Acta.* 601:478–489.

Chernomordik, L. V., G. B. Melikyan, and Yu. A. Chizmadzhev. 1987. Biomembrane fusion: a new concept derived from model studies using two interacting planar lipid bilayers. *Biochim. Biophys. Acta.* 906:309–352.

Clague, M. J., C. Schoh, L. Zech, and R. Blumenthal. 1990. Gating kinetics of pH-activated membrane fusion of vesicular stomatitis virus with cells: stopped flow measurements by dequenching of octadecylrhodamine fluorescence. *Biochemistry.* 29:1303–1308.

de Bruijne, A. W., and J. van Steveninck. 1979. The effect of anesthetics and heat treatment on deformability and osmotic fragility of red blood cells. *Biochem. Pharmacol.* 28:177–182.

Dimitrov, D. S., and A. E. Sowers. 1990*a*. Membrane electroporation-fast molecular exchange by electroosmosis. *Biochim. Biophys. Acta.* 1022:381–392.

Dimitrov, D. S., and A. E. Sowers. 1990*b*. A delay in membrane fusion: lag times observed by fluorescence microscopy of individual fusion events. *Biochemistry.* 29:8337–8344.

Elgsaeter, A., D. M. Shotton, and D. Branton. 1976. Intramembrane particle aggregation in erythrocyte ghosts: the influence of spectrin aggregation. *Biochim. Biophys. Acta.* 426:101–122.

Fricke, H. 1953. The electrical permitivity of a dilute suspension of membrane covered ellipsoids. *J. Appl. Phys.* 24:644–646.

Glaser, R. W., and E. Donath. 1987; Hindrance of red cell electrofusion by the cytoskeleton. *Stud. Biophys.* 121:37–43.

Haywood, A. M. 1987. Entry of enveloped viruses into liposomes. *In* Molecular Mechanisms of Membrane Fusion. S. Ohki, D. Doyle, T. D. Flanagan, S. W. Hui, and E. Mayhew, editors. Plenum Publishing Corp., New York. 427–440.

Heath, B. P., N. Mohandas, J. L. Wyatt, and S. B. Shohet. 1982. Deformability of isolated red blood cell membranes. *Biochim. Biophys. Acta.* 691:211–219.

Herrmann, A., C. Pritzen, A. Palesch, and T. Groth. 1988. The influenza virus-induced fusion of erythrocyte ghosts does not depend on osmotic forces. *Biochim. Biophys. Acta.* 943:411–418.

Huang, S. K., M. Cheng, and S. W. Hui. 1990. Effect of lateral mobility of fluorescent probes in lipid mixing assays of cell fusion. *Biophys. J.* 58:1119–1126.

Knutton, S. 1977. Studies of membrane fusion. II. Fusion of human erythrocytes by sendai virus. *J. Cell Sci.* 28:189–210.

Knutton, S., and T. Bachi. 1980. The role of cell swelling and hemolysis in Sendai virus-induced cell fusion and the diffusion of incorporated viral antigens. *J. Cell Sci.* 42:153–167.

Lang, R. D. A., C. Wickenden, J. Wynne, and J. A. Lucy. 1984. Proteollysis of ankyrin and of band 3 protein in chemically induced cell fusion: Ca^{2+} is not mandatory for fusion. *Biochem. J.* 218:295–305.

Lucy, J. A., and Q. F. Ahkong. 1988. Osmotic forces and the fusion of biomembranes. *In* Molecular Mechanisms of Membrane Fusion. S. Ohki, D. Doyle, T. D. Flanagan, S. W. Hui, and E. Mayhew, editors. Plenum Publishing Corp., New York. 163–179.

Lucy, J. A., and Q. F. Ahkong. 1986. An osmotic model for the fusion of biological membranes. *FEBS (Fed. Eur. Biochem. Soc.) Lett.* 199:1–11.

Lux, S. W. 1979. Spectrin-actin membrane skeleton of normal and abnormal red blood cells. *Semin. Hematol.* 16:21–51.

Marchesi, V. T. 1985. Stabilizing infrastructure of cell membranes. *Annu. Rev. Cell Biol.* 1:531–561.

Mohandas, N., A. C. Greenquist, and S. B. Shohet. 1976. Red cell deformability and spectrin. *Blood.* 48:991*a*. (Abstr.)

Mohandas, N., A. C. Greenquist, and S. B. Shohet. 1978. Effects of heat and metabolic depletion on erythrocyte deformability, spectrin extractibility and phosphorylation. *In* The Red Cell. G. J. Brewer, editor. Alan R. Liss, Inc., New York. 453–472.

Monck, J. R., A. F. Oberhauser, G. A. de Toledo, and J. M. Fernandez. 1991. Is swelling of the secretory granule matrix the force that dilates the exocytotic fusion pore? *Biophys. J.* 59:39–47.

Morris, S. J., D. P. Sarkar, J. M. White, and R. Blumenthal. 1989. Kinetics of pH-dependent fusion between 3T3 fibroblasts expressing influenza hemagglutinin and red blood cells. *J. Biol. Chem.* 264:3972–3978.

Ohno-Shosaku, T., and Y. Okada. 1989. Role of proteases in electrofusion of mammalian cells. *In* Electroporation and Electrofusion in Cell Biology. E. Neumann, A. E. Sowers, and C. A. Jordan, editors. Plenum Publishing Corp., New York. 193–203.

Papahadjopoulos, D., P. R. Meers, K. Hong, J. D. Ernst, I. M. Golstein, and N. Duzgunes. 1988. Calcium-induced membrane fusion: from liposomes to cellular membranes. *In* Molecular Mechanisms of Membrane Fusion. S. Ohki, D. Doyle, T. D. Flanagan, S. W. Hui, and E. Mayhew, editors. Plenum Publishing Corp., New York. 1–16.

Pohl, H. A. 1978. Dielectrophoresis. Cambridge University. Press, London. 579 pp.

Plattner, H. 1989. Regulation of membrane fusion during exocytosis, *Int. Rev. Cytol.* 119:197–286.

Pritzen, C. and A. Herrmann. 1988. Are osmotic forces involved in influenza virus-cell fusion? *Biosci. Rep.* 8:55–64.

Rakow, A. L., and R. M. Hockmuth. 1975. Effect of heat treatment on the elasticity of human erythrocyte membrane. *Biophsy. J.* 15:1095–1100.

Rand, R. P., and V. A. Parsegian. 1986. Mimicry and mechanism in phospholipid models of membrane fusion. *Annu. Rev. Physiol.* 48:201–212.

Sarkar, D. P., S. J. Morris, O. Eidelman, J. Zimmerberg, and R. Blumenthal. 1989. Initial stages of influenza hemagglutinin-induced cell fusion monitored simultaneously by two fluorescent events: cytoplasmic continuity and lipid mixing. *J. Cell Biol.* 109:113–122.

Sekiguchi, K., K. Kuroda, S.-I. Ohnishi, and A. Asano. 1981. Virus-induced fusion of human erythrocyte ghosts: effects of macromolecules on the final stages of the fusion reaction. *Biochim. Biophys. Acta.* 645:211–225.

Sowers, A. E. 1990. Low concentrations of macromolecular solutes significantly affect electrofusion yield in erythrocyte ghosts. *Biochim. Biophys. Acta.* 1025:247–251.

Sowers, A. E. 1989. The mechanism of electroporation and electrofusion in erythrocyte membranes, *In* Electroporation and Electrofusion in Cell Biology. E. Neumann, A. E. Sowers, and C. A. Jordan. Plenum Publishing Corp., New York. 229–256.

Sowers, A. E. 1988. Fusion events and nonfusion contents mixing events induced in erythrocyte ghosts by an electric pulse. *Biophys. J.* 54:619–625.

Sowers, A. E. 1985. Movement of a fluorescent lipid label from a labeled erythrocyte membrane to an unlabeled erythrocyte membrane following electric field-induced fusion. *Biophys. J.* 47:519–525.

Sowes, A. E. 1984. Characterization of electric field-induced fusion in erythrocyte ghost membranes. *J. Cell Biol.* 99:1989–1996.

Sowers, A. E. 1983. Fusion of mitochondrial inner membranes by electric fields produces inside-out vesicles: visualization by freeze-fracture electron microscopy. *Biochim. Biophys. Acta.* 735:426–428.

Spruce, A. E., A. Iwata, J. M. White, and W. Almers. 1989. Patch clamp studies of single cell-fusion events mediated by a viral fusion protein. *Nature (Lond.)* 342:552–558.

Teissie, J., and T. Y. Tsong. 1981. Electric fields induce transient pores in phospholipid bilayer vesicles. *Biochemistry.* 20:1548–1554.

Tsong, T. Y. 1989. Electroporation of cell membranes: mechanisms and applications. *In* Electroporation and Electrofusion in Cell Biology. E. Neumann, A. E. Sowers, and C. A. Jordan, editors. Plenum Publishing Corp., New York. 149–163.

Ungewickell, E., and W. B. Gratzer. 1978. Self-association of human spectrin. A thermodynamic and kinetic study. *Eur. J. Biochem.* 88:379–385.

Vienken, J., U. Zimmerman, R. Ganser, and R. Hampp. 1983. Vesicle formation during electro-fusion of mesophyll protoplasts of *Kalanchoe daigremontiana. Planta (Heidelb.)*. 157:331–335.

Wojcieszyn, J. W., R. A. Schlegel, K. Lumley-Sapanski, and K. A. Jacobson. 1983. Studies on the mechanism of polyethylene glycol-mediated cell fusion using fluorescent membrane and cytoplasmic probes. *J. Cell Biol.* 96:151–159.

Zimmerberg, J., M. Curran, F. C. Cohen, and M. Brodwick. 1987. Simultaneous electrical and optical measurements show that membrane fusion precedes secretory granule swelling during exocytosis of beige mouse mast cells. *Proc. Natl. Acad. Sci. USA.* 84:1585–1589.

Zimmermann, U. 1982. Electric field-mediated fusion and related electrical phenomena. *Biochim. Biophys. Acta.* 694:227–277.